Materials Science and Engineering C 64 (2016) 416–427

Contents lists available at ScienceDirect

Materials Science and Engineering C

journal homepage: www.elsevier.com/locate/msec

Fabrication and characterization of novel nano-biocomposite scaffold of chitosan–gelatin–alginate–hydroxyapatite for bone tissue engineering

Chhavi Sharma [a], Amit Kumar Dinda [b], Pravin D. Potdar [c], Chia-Fu Chou [d], Narayan Chandra Mishra [a,*]

[a] Department of Polymer and Process Engineering, Indian Institute of Technology Roorkee, Roorkee, India
[b] Department of Molecular Medicine and Biology, Jaslok Hospital and Research Centre, Mumbai 400 026, India
[c] Department of Pathology, All India Institute of Medical Sciences, New Delhi 110029, India
[d] Institute of Physics, Academia Sinica, Taipei 11529, Taiwan

ARTICLE INFO

Article history:
Received 20 August 2015
Received in revised form 26 February 2016
Accepted 19 March 2016
Available online 22 March 2016

Keywords:
Natural polymers
Nano-hydroxyapatite
Biocomposite scaffold
Osteoblast
Bone tissue engineering
Foaming

ABSTRACT

A novel nano-biocomposite scaffold was fabricated in bead form by applying simple foaming method, using a combination of natural polymers–chitosan, gelatin, alginate and a bioceramic–nano-hydroxyapatite (nHAp). This approach of combining nHAp with natural polymers to fabricate the composite scaffold, can provide good mechanical strength and biological property mimicking natural bone. Environmental scanning electron microscopy (ESEM) images of the nano-biocomposite scaffold revealed the presence of interconnected pores, mostly spread over the whole surface of the scaffold. The nHAp particulates have covered the surface of the composite matrix and made the surface of the scaffold rougher. The scaffold has a porosity of 82% with a mean pore size of 112 ± 19.0 μm. Swelling and degradation studies of the scaffold showed that the scaffold possesses excellent properties of hydrophilicity and biodegradability. Short term mechanical testing of the scaffold does not reveal any rupturing after agitation under physiological conditions, which is an indicative of good mechanical stability of the scaffold. In vitro cell culture studies by seeding osteoblast cells over the composite scaffold showed good cell viability, proliferation rate, adhesion and maintenance of osteoblastic phenotype as indicated by MTT assay, ESEM of cell–scaffold construct, histological staining and gene expression studies, respectively. Thus, it could be stated that the nano-biocomposite scaffold of chitosan–gelatin–alginate–nHAp has the paramount importance for applications in bone tissue-engineering in future regenerative therapies.

1. Introduction

Globally, approximately 2.2 million bone-grafting procedures are performed every year on the pelvis, spine and other body extremities in attempts to repair or reconstruct the bone [1]. To promote bone growth, surgeons often use bone grafts or substitute materials [2]. Research on bone graft has begun to focus on bone tissue engineering, which involves the combination of cells, scaffold and bioactive agents to engineer new functional tissues that can replace the damaged tissues [3].

Natural bone is a complex of inorganic–organic nanocomposite materials. The primary tissue of bone is relatively hard and mostly made of inorganic material calcium hydroxyapatite [$Ca_{10}(PO_4)_6(OH)_2$] nanocrystallites, which provide rigidity to the bones. The organic part of bone matrix is mainly composed of Type I collagen, an elastic protein which improves fracture resistance and aids in cell growth, proliferation and differentiation [4,5]. Other organic components present in the bone tissue include glycosaminoglycans, osteocalcin, osteonectin, bone sialoprotein and osteopontin. The inorganic matrix of the bone has great strength but is brittle (can break itself), while the organic matrix (e.g., collagen fibers) is flexible and has relatively low strength: inorganic hydroxyapatite and organic collagen (and other materials) together form a matrix that is strong and flexible enough not to be brittle [6,7].

As bone extracellular matrix (ECM) comprises of a variety of components, a scaffold for bone regeneration, if fabricated using single material like nHAp or collagen, cannot provide essential cues for cellular growth. However, two or more materials in combination, if used for scaffold fabrication, might generate a synergistic effect to provide good mechanical strength to the scaffold as well as facilitate cell adhesion, proliferation and differentiation [8–11]. Nowadays, scientists have been focusing on fabricating scaffolds using multi-polymers (more than two polymers) to mimic the properties of ECM, which also consists of multi-polymers [8,12–19]. Here, in this study, we focus on fabricating a composite scaffold with a combination of multi-polymers along with hydroxyapatite, for bone tissue engineering applications.

A scaffold can be fabricated by various techniques, and there are some advantages as well as disadvantages associated with each

* Corresponding author at: Department of Polymer and Process Engineering, Indian Institute of Technology Roorkee, India.
E-mail addresses: chhavisharma19@gmail.com (C. Sharma), amit_dinda@yahoo.com (A.K. Dinda), ppotdar@jaslokhospital.net (P.D. Potdar), cfchou@phys.sinica.edu.tw (C.-F. Chou), mishrawise@gmail.com (N.C. Mishra).

http://dx.doi.org/10.1016/j.msec.2016.03.060
0928-4931/

technique [20,21]. Among the available techniques, the foaming method — generating polymer-foam upon agitation of polymer solution and thereby crosslinking/solidifying the polymer-foam, is one of the simplest and most economic techniques available for scaffold fabrication [8,12,22], but it was not given much attention for tissue engineering applications. That is why we want to explore the foaming method for fabricating multi-polymer composite scaffold. The foaming method applied here is explained in detail in the next section (Section 2).

To fabricate a composite scaffold we selected three polymers, chitosan, gelatin and alginate, and nHAp. The reason for choosing this polymer combination along with nHAp is discussed below.

Although there are many different protein or polysaccharide molecules used in scaffold preparation, chitosan, gelatin and alginate have gained much attention for scaffold fabrication because of their availability, easy handling and low cost [23]. Chitosan is a natural polymer comprising glucosamine and N-acetylglucosamine obtained by the deacetylation of chitin [24]. Since it is degraded by the enzymes of human body, producing non-toxic side products, it is widely used in tissue engineering constructs [25]. Moreover, chitosan has antimicrobial and hemostatic properties [26–28]. Chitosan is osteoconductive, which makes it suitable for engineering hard tissues, but its mechanical properties and biological activities need to be enhanced [29]. For better mechanical properties, chitosan can be modified by blending with other natural polymers like silk, alginate, gelatin or ceramics, such as, tricalcium phosphate and hydroxyapatite [30,31]. Gelatin is a protein derived from collagen and contains Arg-Gly-Asp (RGD) sequences found in ECM, therefore, it promotes initial cell attachment and increases cell spreading, even more than chitosan [32]. Alginate, a naturally occurring polysaccharide, is biocompatible, but it lacks specific cellular interactions, which limits its potential use for wider applications. On the other hand, alginate, in presence of multivalent cations, produces a mechanically strong scaffold [33].

The use of nHAp particles in scaffold fabrication can incorporate nanotopographic features that mimic the nanostructure of natural bone [3,5]. Besides this, nHAp particles can provide the scaffold good mechanical strength, which is a prerequisite of the scaffold to be applied for bone regeneration [6]. The presence of nHAp in the scaffold also has a strong influence on bone regeneration [23,24].

Thus, if chitosan, gelatin, alginate and nHAp are combined all together during scaffold fabrication then this combination would impart the scaffold higher mechanical strength and biological similarity to the natural bone. Therefore, the specific goal of the present study is to fabricate a chitosan–gelatin–alginate–nHAp composite scaffold by exploring the simplest foaming method using commercially available nHAp to (i) improve the mechanical properties of the composite scaffolds relative to chitosan–gelatin–alginate scaffolds and (ii) to evaluate the biological performance of the nHAp incorporated scaffold for bone tissue engineering applications. To the best of our knowledge, this polymer combination along with nHAp is novel and has not been used before for scaffold fabrication.

2. Materials and methods

2.1. Fabrication of nano-biocomposite scaffold

Fig. 1 explains the fabrication of nHAp–chitosan–gelatin–alginate composite scaffold by the foaming method without using any surfactant. Solutions of 2 wt% alginate (Acros Organics, New Jersey, U.S.A.) and 5 wt% gelatin (Merck Specialities Pvt. Ltd., Mumbai) were prepared in sterilized water, and mixed in the ratio of 1:1. Thereafter, $NaHCO_3$ (0.9%), a gas generating agent, was added to this mixture and was continuously stirred for 2 h whereby foam is generated. Next, 0.025% glutaraldehyde solution (SD Fine-Chem. Ltd., Mumbai, India), crosslinker for chitosan [34] and gelatin, was added to the alginate–gelatin–$NaHCO_3$ foam matrix with a volume ratio of 1:40, and allowed to react (or crosslink) with the mixture for 10 h under the condition of continuous agitation. On addition of glutaraldehyde to this polymer mixture (Step 2 in Fig. 1), aldehyde groups present in glutaraldehyde, were believed to crosslink with the amino groups of gelatin present in the mixture [8,35]. Because of the continuous agitation, foam was generated in a large volume. The polymer foam was extruded drop-wise into a solution

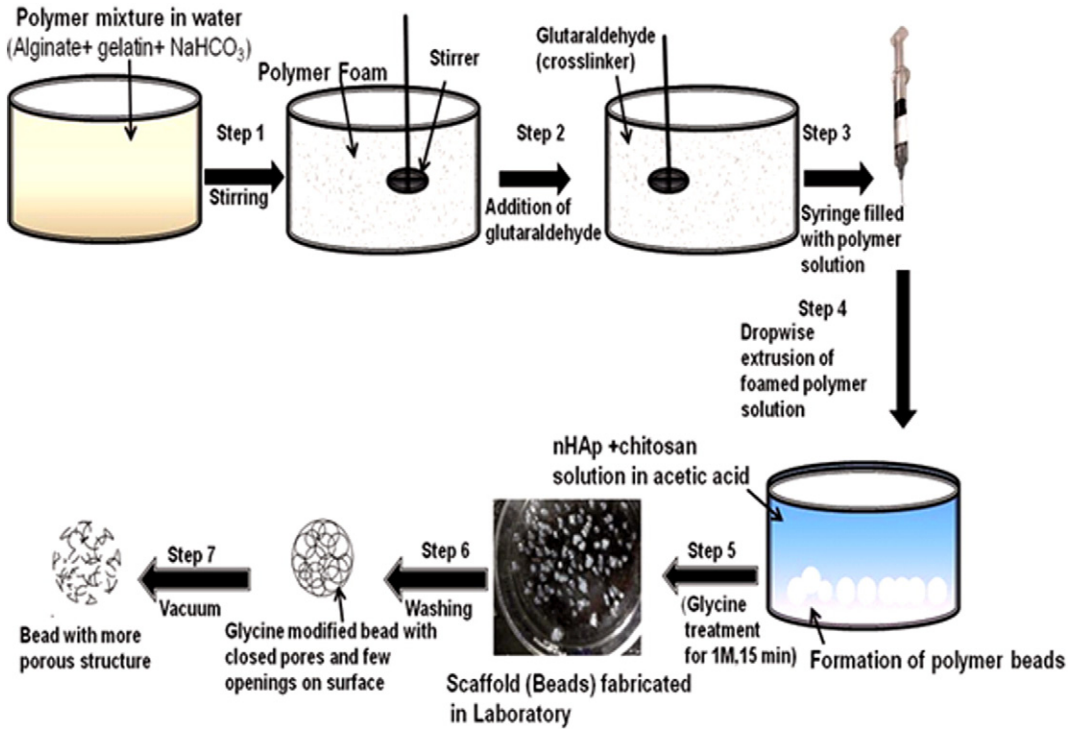

Fig. 1. Schematic representing fabrication of nHAp–chitosan–gelatin–alginate composite scaffold by foaming method.

containing nHAp (Sigma, St. Louis, MO, U.S.A.) particles dispersed in chitosan solution(MW 100,000–300,000; Sigma, St. Louis, MO, U.S.A.), which resulted in scaffold in bead form. Here, the nHAp particles were dispersed in chitosan solution by sonicating the mixture of nHAp particles (1 wt% in sterilized water) and chitosan solution (2 wt% in 1 wt% acetic acid) mixed in 1:1 volume ratio.

The beads were allowed to remain in solution for 12 h, to facilitate efficient crosslinking among alginate, gelatin, chitosan and nHAp, and then the beads were washed with sterilized water 20 times, to remove excess glutaraldehyde. Scaffolds were then modified by immersing the scaffold in glycine (Himedia, Mumbai, India) solution (1 M) for 15 min, in order to block free aldehyde groups if any remained in the scaffold. After glycine treatment, scaffolds were washed with sterilized water twice. Finally, the scaffold beads were exposed to vacuum for 12 h to create more porous structures inside. The fabricated scaffold was characterized and evaluated for bone tissue engineering applications.

Here, it is pertinent to mention that initially the pH of the solution of alginate, gelatin and $NaHCO_3$ was 7 where gelatin was at isoelectric point with no charge. It is expected that no interaction between alginate and gelatin occurred in the initial stage.

We prepared chitosan solution in acetic acid and chitosan is positively charged. If we add chitosan solution initially, then it will be acidic, and alginate will precipitate immediately. Besides, gelatin will be positively charged in acetic acid solution, and chitosan and gelatin, both, will crosslink with alginate to form gel, which will prevent foaming. That is why chitosan was added later.

2.2. Scaffold characterization

2.2.1. Scaffold size and morphology

The diameter of nHAp–chitosan–gelatin–alginate scaffold beads was determined by taking images of scaffold beads by a stereo microscope (Olympus, Tokyo, Japan) under 4X magnification and 50 beads were measured from these photographs using a computational Image J program (NIH, Bethesda, Maryland, U.S.A.).

Morphology of composite scaffolds was studied by using an environmental scanning electron microscope (ESEM) (Quanta 200, FEI, Netherland) as described in previous literature [8]. Each time, 5 beads prepared from independent experiments, were examined. The size of the pores was determined for the 30 bead images by using Image-J analysis software, and the average pore size was calculated.

2.2.2. Energy Dispersive X-ray Spectroscopy (EDS)

Chemical analysis of scaffold samples was performed with a LEO 1525 scanning electron microscope equipped with an EDX detector. To quantify the chemical content of small areas (~60 μm^2) on the sample surface, distinctly different topographical areas were chosen from the sample and examined at 10 kV using INCA Energy 3000 software.

2.2.3. Fourier transform infrared spectroscopy (FT-IR)

Fourier transform infrared spectroscopy (FTIR) is an important tool to carry out semi-quantitative functional analysis and to investigate intermolecular interaction between different compounds. Infrared (IR) spectra were recorded with a Nexus Thermo FTIR spectrophotometer (Nicolet Co.) as described in previous literature [8,12].

2.2.4. Porosity

Porosity is defined as the percentage of void space in a solid and it is a morphological property independent of the material [36]. The porosity of composite beads was determined by liquid displacement method. In brief, beads were placed in a graduated cylinder filled with a known volume of ethanol (V_1). The total volume following bead immersion was recorded (V_2). The beads were removed with the volume V_T whereby, solvent is entrapped in the pores, and the remaining volume of ethanol in the graduated cylinder was denoted by (V_3). The total volume (V_T) of the beads was calculated according to Eq. (1)

$$V_T = V_2 - V_3. \tag{1}$$

The porosity χ was determined using the following equation:

$$\chi = \frac{V_1 - V_3}{V_T} \times 100. \tag{2}$$

The porosity-determination experiment was repeated 6 times, and the mean porosity was calculated.

2.2.5. Swelling ratio

Hydrophilicity of the scaffold serves as one of the imperative features in the evaluation of biomaterials for tissue engineering because it is critical for the absorption of body fluid and for the transport of cell nutrients and metabolites. The swelling gives a measure of hydrophilicity and it is defined by the following equation:

$$S = (w_s - w_d)/w_d) \times 100\% \tag{3}$$

where, S = percentage swelling, w_s = wet weight of the bead-scaffold after swelling, and w_d = weight of the bead-scaffold after drying. Briefly, the beaded scaffolds were immersed in phosphate buffer saline (PBS) (Sigma, St. Louis, MO, U.S.A.) (pH = 7.4) at room temperature for an hour. After a one hour immersion, in every 10 min, a known quantity of the bead-scaffolds was retrieved and excess water was removed using filter paper. The wet weight of the scaffold (w_s) was determined using an electronic balance, after which the swollen scaffold was dried in an oven at 50 °C for half an hour, and the dry weight (w_d) was measured. Each time, the percentage swelling (S) was calculated from the values of w_s and w_d. The experiment was carried out until the time point, where no further swelling of beads was observed and the equilibrium point of swelling of beads was determined. The experiment was repeated 6 times individually. The maximum volume of the beads after swelling was also calculated based on the diameter of the beads after swelling by applying the formula as given below:

$$\text{Volume of bead} = \frac{1}{6}\pi d^3 \tag{4}$$

where, d = diameter of the swelled bead.

2.2.6. Evaluation of mechanical stability

A short term stability assay was carried out to study the behavior of the beads submitted to a combination of destabilizing forces so as to mimic the physiological conditions. The procedure was based on Orive et al. with some modifications [37]. Briefly, 10 beads were taken in a beaker containing 10 ml of PBS (pH = 7.4) and the beaker was placed in a shaker at 200 rpm at room temperature. The beads from the beaker were examined under a stereo microscope after 48 h. Results are expressed as the percentage of ruptured beads as a function of time and the stereo microscopy images showing ruptured beads after 48 h. The mechanical strength of the glycine treated collagen/chitosan microspheres was also determined in previous studies after 48 h of agitation by a similar method [38].

2.2.7. In vitro enzymatic degradation

Degradability of the scaffold was determined by mass change of scaffold beads after their incubation in 1 ml 1X PBS (pH 7.4) containing 1.6 μg/ml of lysozyme (100,000 U/mg) (Himedia, Mumbai, India) [39]. A known quantity (w_i = 0.5 g) of freshly prepared beads was taken in a tissue culture plate in triplicate. To determine the degradation profile, the beads were removed from lysozyme solution in 1X PBS after the 1st, 3rd, 5th, 7th, 14th, 21st and 28th days, thoroughly washed with distilled water and dried and weighed (w_f). The extent of the in vitro

degradation was calculated as the percentage of weight difference of the scaffold before and after hydrolysis with the lysozyme solution by the following equation.

$$\%\ \text{weight loss} = \frac{w_i = w_f}{w_i} \times 100 \quad (3)$$

2.3. Cell behavior on the scaffold

2.3.1. In vitro cell culture using osteoblast cell line

Osteoblast cells (received from Jaslok Hospital and Research Centre, Mumbai, India) were cultured in Dulbecco's modified eagle medium (DMEM) (Sigma, St. Louis, MO, U.S.A.) growth media supplemented with 10% FBS, penicillin (100 units/ml) and streptomycin (100 μg/ml), 2 μl/ml glutamine, and 12 μl/ml insulin in an incubator at 37 °C with 5% CO_2 supply. The Subconfluent cultures of osteoblasts from 50 mm culture flask were detached by trypsinization using 0.25% Trypsin–Ethylenediaminetetraacetic acid (EDTA) solution (Sigma, St. Louis, MO, U.S.A.), resuspended in complete growth medium and the cell counting was done by using a hemocytometer (Chemometec, Denmark).

For MTT experiments, 1×10^3 cells of osteoblast cells were plated per well in triplicate with and without scaffold in 96 well plates (1 bead/well) and fed with respective growth medium. The culture plates were incubated for 1, 3, and 5 days at 37 °C in a CO_2 incubator for a respective period. The experiment was terminated at respective intervals and cells were further processed for MTT analysis. One scaffold was put in each well having 1×10^3 osteoblast cells for this experiment.

2.3.2. Cell viability, proliferation and attachment over the scaffold

Cytotoxicity assay of the composite scaffold was performed in order to investigate the viability and proliferation of cells over the scaffold. Human osteoblast cells were used to check the compatibility of scaffold for the bone tissue engineering. Prior to cell seeding, the scaffolds were sterilized by exposing to UV light from a mercury arc lamp source under the laminar flow hood. Scaffolds were then placed in a tissue culture plate and soaked with 100 μl DMEM overnight at 37 °C in a CO_2 incubator to make the scaffold surface more efficient for cell attachment. Scaffolds were placed in 96 well tissue culture wells (1 bead/well) in triplicate and incubated with osteoblast cells at 3 time points e.g. 1, 3 and 5 days at 37 °C in a CO_2 incubator in order to test the toxicity of leachable from the scaffold towards human osteoblast cells along with control cell without scaffold. After the incubation, the medium was removed and 90 μl of fresh complete growth media was added to the wells. Then 10 μl of 3-(4,5-dimethylthiazol-2-yl-2,5-diphenyltetrazolium bromide) (MTT) (Himedia, Mumbai, India) solution (5 mg/ml stock in 1X PBS) was added to the media to make final volume of 100 μl. The plates were incubated at 37 °C for 4 h until purple formazan crystals were formed due to reduction of MTT by viable cells. The media and beads were removed from the well and 200 μl of dimethyl sulfoxide (DMSO) (Himedia, Mumbai, India) was added to each well to dissolve the formazan crystals. Absorbance was taken on a Biorad ELISA plate reader at 490 nm with the subtraction for plate absorbance at 620 nm. The absorbance is directly proportional to the amount of metabolically active cells. The results were expressed by comparing the absorbance values of cell–scaffold construct with the control values.

To check the morphology of the cells and the scaffold interaction, the cell seeded scaffolds were fixed with glutaraldehyde (2.5%) at 4 °C for 6 h and then rinsed with PBS and both were observed under an ESEM.

Phase-contrast microscopy for the acquisition of cell images was carried out with cultured osteoblast cells on composite scaffold. After the incubation of cells with scaffold, the cell–scaffold constructs were viewed under an inverted phase-contrast microscope (Zeiss) and photographed.

2.3.3. Histology of osteoblast cells in the presence of scaffold

The osteoblast cell cultures were set up in 48 well plates to study the morphological features of these cells. Histological staining of these cells was performed after incubation of these cells with scaffold for 5 days at 37 °C in a CO_2 incubator. The cell–scaffold constructs were subjected to three different stains to reveal their morphological phenotype of bone cells as mentioned below. For each stain, 6 individual cell–scaffold constructs were examined under a phase contrast microscope and photographed.

2.3.3.1. Alizarin Red staining. Alizarin Red is used in a biochemical assay to determine, the presence of calcific deposition by cells of an osteogenic lineage. As such, it is a marker of matrix mineralization which is a decisive step towards the formation of calcified extracellular matrix associated with bone [40]. For osteogenesis studies, osteoblast cells were cultured for 5 days with a composite scaffold. Alizarin Red staining of cell–scaffold constructs was performed as mentioned in previous literature [40]. After staining, the cell–scaffold constructs were washed with distilled water 4–5 times and examined under a phase contrast microscope and photographed.

2.3.3.2. Giemsa staining. Giemsa staining was done to ensure whether the osteoblasts retain their characteristic shape i.e., large cells with prominent spherical nuclei as expected and reported [41] even in the presence of scaffold. The osteoblast cells were cultured for 5 days with a composite scaffold and stained, following the protocol mentioned previously [41]. The stained cells over the scaffold were observed under a phase contrast microscope and photographed.

2.3.3.3. Oil Red staining. Oil Red staining was perform to verify that osteoblasts were not differentiated in vitro into adipocyte cells (that gives Oil Red staining positive) and retained their osteoblastic phenotype in the presence of the scaffold. The osteoblast cells were cultured for 5 days with a composite scaffold. The cells on the scaffold were fixed with 50% methanol for 1 h at room temperature. Now, 2 ml of 60% isopropanol was added to it for 5 min. After this, Oil Red stain (Fisher Scientific, Mumbai, India) was applied to the cell–scaffold construct for 5 min. The construct was washed with distilled water and examined under a phase contrast microscope and photographed.

2.4. Gene expression study

2.4.1. Molecular marker expression in osteoblast cell–scaffold construct

Molecular markers are very important to understand the phenotypic changes that occur in the cells when treated or exposed with any chemical or biological material [42]. In this study, we have studied specific genes that are expressed specifically by human osteoblast (bone) cells by using reverse transcriptase polymerase chain reaction (RT/PCR) technology. RT/PCR analysis was carried out by using specific primers (Table 1) for respective genes, as described previously [43,44]. This study has shown how osteoblast cells respond on the molecular level to the composite scaffold. We have used human osteoblast cell line, which is developed and characterized by Dr. Potdar at Jaslok Hospital and Research Centre, Mumbai, India [43]. We have selected CD105 and CD73 as mesenchymal stem cell markers, CD34 as a hematopoietic marker. Keratin 18, CD44 and osteocalcin (OCN) are osteoblastic markers. We have selected OCN marker to confirm the osteogenic characteristics of the human osteoblastic cell line. β-Actin has been used as a housekeeping gene in this study.

2.4.2. RNA extraction

In this study, we have studied specific genes that are expressed specifically by human osteoblast (bone) cells by using RT/PCR technology. The phenotypic expression of these cells was checked in the presence and absence of scaffold. 1×10^3 cells of human osteoblast cells per scaffold were plated in each 48 well plate with and without scaffold. We

Table 1
Primer sequences used for gene expression studies for human osteoblast cells.

S. No	Molecular marker	Forward primer 5′ ➔ 3′ Reverse primer 5′ ➔ 3′	Product size (bp)
1. 1	CD105	TGTCTCACTTCATGCCTCCAGCT AGGCTGTCCATGTTGAGGCAGT	378
2. 2	CD73	CACCAAGGTTCAGCAGATCCGC GTTCATCAATGGGCGACCGG	1003
3. 3	CD44	CAACCCTACTGATGATGACG GGATGCCAAGATCATCAGCC	312
4. 4	CD34	GCAAGCCACCAGAGCTATTC GGTCCCAGGTCCTGAGCTAT	198
5. 5	Keratin 18	GAGATCGAGGCTCTCAAGGA CAAGCTGGCCTTCAGATTTC	357
6. 6	OCN	GGTGCAGCCTTTGTGTCCAAGC GTCAGCCAACTCGTCACAGTC	115
7. 7	β-Actin	AACCCCAAGGCCAACCGCGGAG AAGATGACC GGTGATGACCTGGCCGTCAGGC AGCTCGTA	417

have put 4 scaffolds in each well in triplicate to get sufficient cells for RNA extraction. The cells were incubated at 37 °C in a CO_2 incubator for 5 days by observing morphological changes every day by phase contrast microscopy. The cultures were terminated after 5 days and then washed with 1X PBS solution and then transferred into 500 μl of Trizol solution (SD Fine-Chem. Ltd., Mumbai, India) for RNA extraction. The time matched control cells (incubated without scaffold) were also harvested after 5 days. Total RNA was extracted using Trizol reagent and total RNA was then quantified by using a spectrophotometer at 260 & 280 nm wavelengths. The purity of each sample was observed using the A260/A280 ratio. A ratio of 1.8–2.0 was considered as purified RNA sample. Extracted RNA was then stored in diethylpyrocarbonate (DEPC) water at −85 °C till further molecular analysis.

2.4.3. Synthesis of cDNA from extracted RNA

Complementary DNA (cDNA) synthesis was performed using a commercially available cDNA kit (Applied Biosystems U.S.A.). Two micrograms of extracted RNA was reverse transcribed by using MuLV reverse transcriptase to generate full-length first strand cDNA from total RNA extracted from osteoblast cells. Further, the synthesized cDNA was used as a template for polymerase chain reaction (PCR) amplification to study gene expression in these cells. The PCR product was successfully amplified in all genes using Taq polymerase (Invitrogen, U.S.A.) and the product obtained was loaded on 2% agarose gel, visualized under a gel documentation system (Model — Alpha Imager HP, Cell Bioscience) and photographed.

3. Results and discussion

3.1. Scaffold fabrication

We have successfully fabricated a tissue engineering scaffold from the combination of natural origin polymers — chitosan, gelatin, alginate and a bioceramic — nHAp, by applying the foaming method without using any surfactant [Fig. 1, Section 2.1]. This polymer combination helped in stabilizing foam for a long time (above 50 min) — a prerequisite for scaffold fabrication by the foaming method [12].

During the scaffold bead formation, alginate interacts/crosslinked with both Ca^{2+} ions and chitosan, and beads were formed. Ca^{2+} ions present in the solution of acetic acid containing chitosan and nHAP (Step 4 in Fig. 1), served to ionically crosslink alginate.

Some of the chitosan molecules present in gelling solution (Step 4 in Fig. 1), might also bond to alginate weakly, forming a polyelectrolyte complex due to electrostatic interactions between oppositely charged groups ($—COO^-$ of alginate and $—NH^{+3}$ of chitosan). The polyelectrolyte complex formation between chitosan and alginate, was also reported previously [8,45]. Here, the free aldehyde groups of glutaraldehyde molecules, were supposed to crosslink with amino groups of chitosan by forming imine bond ($^-C{=}N$), following the cross-linking reaction. The formation of imine bonds between aldehyde groups of glutaraldehyde and amine groups of chitosan by covalent linkage, was also reported earlier [46]. Thus, glutaraldehyde crosslinks both chitosan and gelatin in different stages of scaffold formation. It is supposed that the possible interactions between the Ca^{2+} and $PO4^{3-}$ groups of HAp and the $—COO^-$ and $—NH^{+3}$ groups of gelatin and chitosan respectively, have also occurred that led to a successful formation of nanocomposite bead scaffold. These interactions were further corroborated by FTIR studies (Section 3.4) and were also reported in the earlier studies [47, 48].

The acetic acid reacts with $NaHCO_3$ to evolve CO_2 from inside the bead, promoting high porosity in the bead-scaffold.

3.2. Scaffold size and morphology

The size of 50 scaffold-beads was measured by using Image-J software (Java version) and the diameter of the beads is found to be in the range from 1 to 3 mm with an average size of 2 ± 0.5 mm.

Fig. 2(A–H) showed ESEM images of the composite scaffold. The scaffold is porous and the pores were spread over the entire scaffold; nHAp particles were well distributed over the pore walls of the scaffold as indicated by arrow marks in the ESEM images. The surface of the scaffold appears to be rough due to the nHAp particles impregnated over the scaffold surface. The pore size of the composite scaffold is in the range of 10–264 μm with the mean size of 112 ± 19.0 μm. The large pores in the scaffold will facilitate the osteoblast cells to fit better inside the scaffold leading to direct osteogenesis without proceeding towards cartilage formation [36], while the smaller pores (10–25 μm) are supposed to facilitate nutrient diffusion throughout the scaffold [48]. In some studies it has been observed that smaller pores play a crucial role in nutrient diffusion, cell growth and proliferation [49]. Smaller pores provide either a larger surface area or a geometrically more suitable substrate for angiogenic and/or osteogenic protein adsorption and cell anchorage, leading to the more rapid induction of angiogenesis and thus bone apposition [49]. Cross section of the scaffolds was also examined as shown in Fig. 2(E–H). Sectioned beads also revealed porous structures with nHAp particles embedded on it. Thus, the composite scaffold possesses sufficiently porous morphology with nHAp distribution that makes the scaffold vital for bone tissue engineering applications.

3.3. Energy Dispersive X-ray Spectroscopy (EDS)

Chemical analysis by EDS is done to characterize the constituents of the composite scaffold. EDS analysis (Fig. 3) showed that the scaffold surface consists of carbon (C) and oxygen (O) as detected by the specific peaks. The core portion of the scaffold typically consists of calcium (Ca) and phosphorous (P), and therefore similar to the nHAp phase.

3.4. Fourier transform infrared spectroscopy (FT-IR)

FT-IR spectra of (a) chitosan; (b) alginate; (c) gelatin; (d) composite scaffold; and (e) nHAp powder were shown in Fig. 4. The IR spectrum of chitosan confirms the presence of O–H and N–H stretching vibration at 3442 cm^{-1}, in which the –OH stretching vibration is overlapped by N–H stretching. The band at 1641 cm^{-1} corresponds to N–H bending vibrations of secondary amide. The C–O–C bending, C–O bending and C–OH bending were visible at 1173 cm^{-1}. The C–H bending was seen at 1378 cm^{-1}. The band at 900 cm^{-1} corresponds to the saccharide structure of chitosan [24].

The IR spectrum of alginate showed characteristic bands for its glucuronic (G) and mannuronic (M) acid units at 1031 cm^{-1} and 1091 cm^{-1}, respectively. The –OH stretching band was observed at 3407 cm^{-1}. The H–C–H and O–C–H stretching vibration was seen at

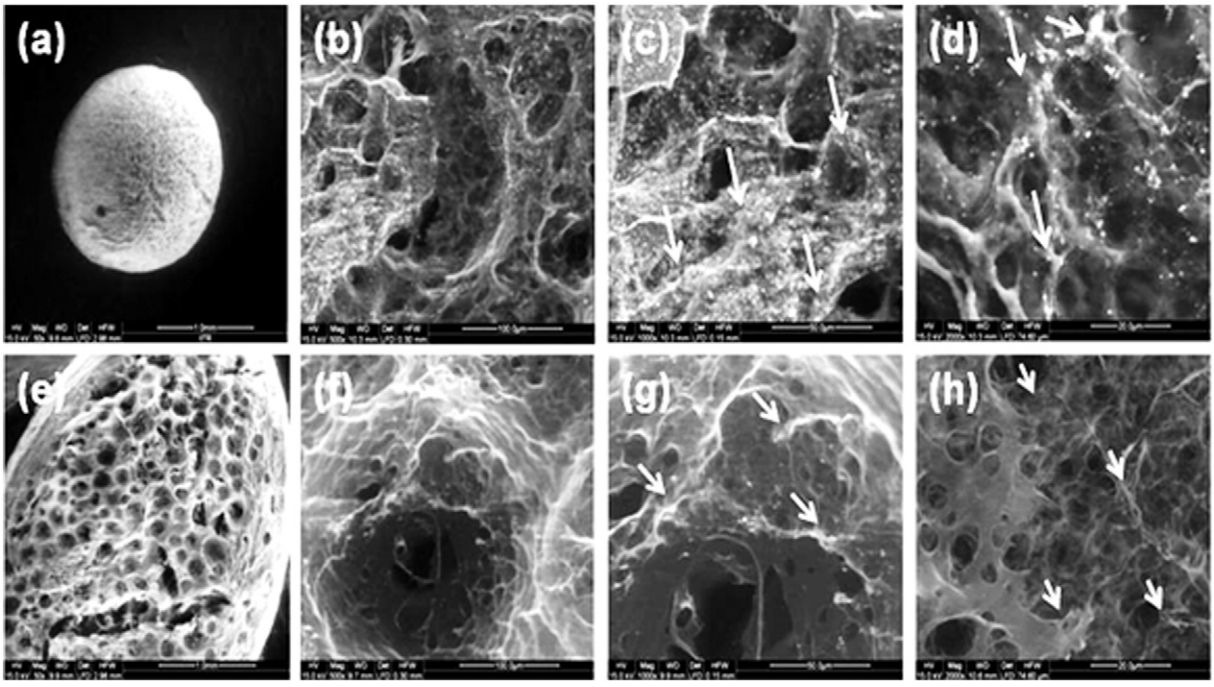

Fig. 2. Scaffold morphology by ESEM analysis: (A,B,C,D) — nHAp–chitosan–gelatin–alginate composite scaffold at 50X, 500X, 1000X and 2000X, respectively; (E,F,G,H) — cross-section of composite scaffold at 50X, 500X, 1000X and 2000X, respectively. The nHAp particle distribution is clearly visible on the scaffold surface (B,C,D) as well as in the cross-section(F,G,H) of the scaffold.

1416 cm^{-1}. The $-COO^-$ stretch was visible at 1610 cm^{-1}. The bands at 886 cm^{-1} and 818 cm^{-1} indicate β-glycosidic linkages between G and M units of alginate.

The IR spectrum of gelatin showed a band at 3443 cm^{-1} due to N–H stretching of secondary amide and N–H out-of-plane wagging at 665 cm^{-1}. The pure gelatin revealed a series of amide (1240 cm^{-1}, 1543 cm^{-1}, and 1650 cm^{-1}) and carboxyl (1300–1450 cm^{-1}) bands, which were attributed to the amino acids of gelatin backbone, such as glycine, proline, and hydroxyproline [50].

In the FTIR spectrum of nHAp, a sharp band appearing at approximately 3572 cm^{-1} indicates O–H stretching. A $PO4^{3-}$ stretching peak appeared at 1030 cm^{-1} and $PO4^{3-}$ bending vibrations appeared at 604 cm^{-1} and 563 cm^{-1}. The small peak at 860 cm^{-1} can be attributed to symmetric P–O stretching vibration [24].

The IR spectrum of polymeric composite beads showed a band at 1632 cm^{-1} which corresponds to imine bond (–C=N) which might be formed between gelatin and glutaraldehyde as well as chitosan and glutaraldehyde present in the polymer mixture. This peak was not observed in FT-IR of pure gelatin and chitosan. This implies the possibility of crosslinking reactions among chitosan, gelatin and glutaraldehyde molecules during scaffold formation [8,48].

The band of the amino group (1173 cm^{-1} seen in pure chitosan) is absent in the composite scaffold. This is an indication of a possible interaction between the chitosan and nHAp during scaffold fabrication. The band of P–O at 1030 cm^{-1} and 604 cm^{-1} in nHAp has shifted to 1033 cm^{-1} and 628 cm^{-1} after composite formation, which evidences that the P–O groups of nHAp have taken part in bonding particularly with the NH_3^+ groups of chitosan present in the scaffold. The interaction between the P–O group of nHAp and NH_3^+ groups of chitosan was also reported previously [51]. Shifting of the bands in FTIR of composite scaffold revealed that there exists some chemical bonding at the nHAp–polymer interface.

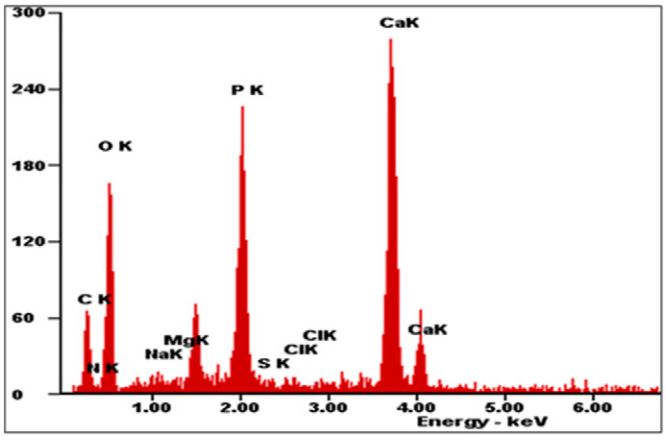

Fig. 3. Elemental analysis of nHAp–chitosan–gelatin–alginate composite scaffold determined by EDS.

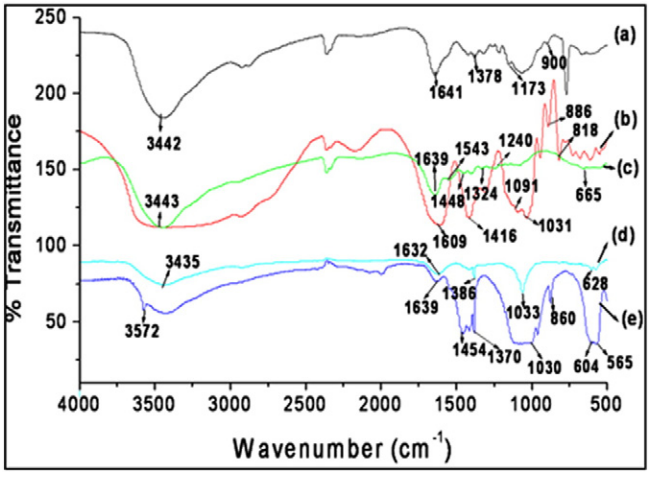

Fig. 4. FTIR spectra of (A) chitosan; (B) alginate; (C) gelatin; (D) nHAp–chitosan–gelatin–alginate composite scaffold; and (E) nHAp.

3.5. Porosity

Porosity of the nHAp–chitosan–gelatin–alginate composite scaffold is about 82% (mean porosity 80.8% ± 1.20). In an earlier study, glycine modified chitosan–gelatin–alginate scaffolds showed a porosity of about 90% (mean porosity of 91.8 ± 1.90%) [8,12]. The decrease in porosity (~11%) in the nHAp–chitosan–gelatin–alginate composite scaffold is probably due to the deposition of nHAp over the scaffold that has made the surface of the scaffold uneven and patchy (Fig. 2). This result is consistent with another study by Kim and coworkers [51], who reported a decrease in porosity by the addition of hydroxyapatite in the gelatin scaffold. The decrease in porosity may be attributed to the interactions particularly between $-NH_3^+$ groups of chitosan and both –OH groups of nHAp as well as Ca^{2+} ions of nHAp [50]. The nHAp addition has decreased the porosity but still the porosity (82%) is sufficiently enough to facilitate the cell seeding and nutrient diffusion throughout the whole structure of the scaffold.

3.6. Swelling ratio

As shown in Fig. 5, the swelling ratio of nHAp–chitosan–gelatin–alginate composite scaffold beads, after immersion in PBS for 10 min, is 400% and thereafter it (swelling ratio) increases with time, which reflects the good hydrophilicity of the scaffold. As after 60 min, no further swelling of the beads (negligible swelling effects) was observed, which indicates that the equilibrium point of swelling was reached at approximately 940%. Though, the scaffold showed good degree of swelling but the swelling is less compared to chitosan–gelatin–alginate scaffold in which the equilibrium point of swelling was observed at about 1030% in 60 min as reported in our previous article [8]. This reflects that the addition of nHAp has affected the swelling property of the scaffold. This result is consistent with other studies in which the addition of nHAp and tricalcium phosphate in scaffold fabrication has resulted in decreased swelling ratio [52]. Overall, the scaffold is hydrophilic which indicates that the nHAp–chitosan–gelatin–alginate composite scaffold can be applied potentially for tissue engineering applications as the hydrophilic nature of the scaffold will facilitate the absorption of body fluid, which consists of water mainly and is important for the diffusion of nutrient and metabolites.

We have also calculated the maximum volume of the beads (Table 2) after swelling because this will help us for application of the scaffold in clinical trial by knowing the size of the tissue defect. The final diameter of the beads after swelling is in the range of 2.5 mm to 4.7 mm with an average of 3.7 ± 0.8 mm as measured by Image J software. The maximum swelling volume was in the range from 8.18 mm^3 to 54.4 mm^3 (for swelled beads of diameter 2.5 mm to 4.7 mm) as shown in Table 2.

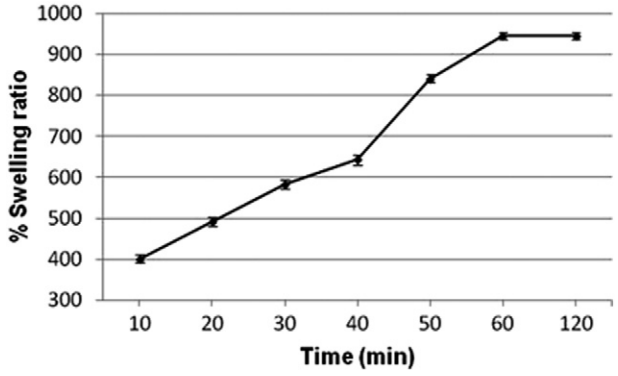

Fig. 5. Swelling ratio (%) of nHAp–chitosan–gelatin–alginate composite scaffold.

3.7. Evaluation of mechanical stability

A short term mechanical stability assay was carried out by exposing the nHAp–chitosan–gelatin–alginate composite scaffold beads to both agitation and osmotic swelling pressure in PBS solution under physiological conditions. By this study, it was demonstrated that at the end of 48 h of agitation, the beads showed no deformation in shape and no rupturing (Fig. 6), which indicates good mechanical stability of the scaffold under physiological conditions. Contrary to this, the chitosan–gelatin–alginate scaffold showed deformation and slight rupturing after 10 h of agitation [8] and thereafter the rupturing increased with increasing agitation time. The mechanical strength of the chitosan microspheres was also determined in previous studies after 48 h of agitation by a similar method [53].

The increased mechanical stability of the nHAp–chitosan–gelatin–alginate composite scaffold was possibly due to the presence of nHAp that is known to produce mechanically stronger scaffolds [54]. The interactions among nHAp, chitosan, gelatin and alginate might also have resulted in increased mechanical stability. At physiological pH, gelatin and alginate are anionic while chitosan is cationic in nature. Thus, they exhibit an electrostatic interaction. Moreover, there will be the possible interactions among the NH_3^+ group of chitosan with Ca^{2+}, $PO4^{3-}$ ions and –OH groups of nHAp as reported by several scientists [51,55]. Thus, all these interactions provided additional crosslinking among the polymers (chitosan, gelatin, alginate) and nHAp, which might be responsible for the formation of more compact and mechanically stable scaffold structure.

3.8. In vitro enzymatic biodegradation

The degradation of the nHAp–chitosan–gelatin–alginate composite scaffold was studied in PBS–lysozyme solution. It was found that there is no degradation up to day 3 and from day 5th the scaffold starts degrading (Fig. 7). The degradation of the composite scaffold after 28 days was found to be 35% only. However, the chitosan–gelatin–alginate composite scaffold showed approximately 70% degradability only after 21 days under the same physiological condition [8,12]. This indicates that the addition of nHAp reduced the rate of degradation of the nHAp–chitosan–gelatin–alginate composite scaffold to a great extent. This result might be attributed to the formation of more stable and compact scaffold structure formed by the interactions among the polymers (chitosan, gelatin, alginate) and nHAp. The degradation result is consistent with other studies in which the reduced degradation was observed in hydroxyapatite based scaffolds [56,57,58]. The reduced degradation rate of the scaffold might be beneficial as it can provide sufficient time for the formation of neotissue and ECM during tissue regeneration.

3.9. Cell behavior on the scaffold

3.9.1. Cell viability, proliferation and attachment over the scaffold

MTT assay was performed for 1, 3 and 5 days to evaluate the cell viability and proliferation of osteoblast cells over the nHAp–chitosan–

Table 2
Table showing size of beads with different radii.

Average diameter of scaffold beads before swelling (in mm)	Average diameter of scaffold beads after swelling (in mm)	Volume of beads after swelling (in mm^3)
1	2.5	8.18
1.5	3	14.1
2.0	4.1	36.1
2.5	4.3	41.6
3	4.7	54.4

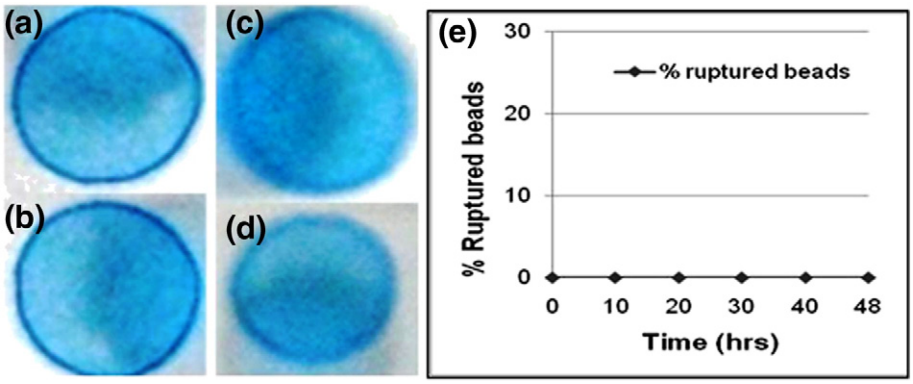

Fig. 6. nHAp–chitosan–gelatin–alginate composite beads before agitation (A,B); composite beads after 48 h agitation (C,D) under physiological conditions (magnification: 20X for all images);(E) percentage of ruptured beads in PBS as a function of time.

gelatin–alginate composite scaffold as well as on the chitosan–gelatin–alginate scaffold without nHAp incorporation. Cells seeded on a tissue culture plate without scaffold, were taken as a control. The absorbance values i.e., optical density (O.D.) was measured for the cell-seeded scaffold and the O.D. is proportional to cell viability. The chitosan–gelatin–alginate composite scaffold showed an increase in cell viability and proliferation with time as indicated by the absorbance values which are higher than the absorbance values of the control (Fig. 8). However, the nHAp–chitosan–gelatin–alginate scaffold showed a significant increase in cell proliferation compared with the chitosan–gelatin–alginate scaffold, which does not contain nHAp (Fig. 8). The better proliferation of the osteoblasts over the nHAp–chitosan–gelatin–alginate composite scaffold is believed to be due to higher attachment of cells over the composite scaffold. The higher attachment might be due to the presence of nHAp particles and the roughness provided by nHAp particles. The higher osteoblast cell viability for scaffold fabricated with nHAp was also reported by several scientists [24,50,52].

Fig. 9(A–F) showed that the osteoblast cells adhered to the nHAp–chitosan–gelatin–alginate composite scaffold surface after 1, 3 and 5 days of incubation with the scaffold. After 1 day, it was observed that the cells adhere to the scaffold and the shape of the cells is mostly rounded. Cells grow with time, spread over the scaffold, and after 3 and 5 days, the cells were observed to have a spindle to polygonal morphology with the cell-membrane being quite flattened onto the rough surface of the scaffold created by the nHAp particles (Fig. 9(C—F)). This type of morphology of osteoblast cells was reported previously on the titanium based scaffold [59]. The results proved that the nHAp incorporated chitosan–gelatin–alginate scaffold provided a very good environment for the adhesion and proliferation of osteoblast cells. The nHAp particles, its nanofeatures and rough surface are believed to be the main boosting factors responsible for the good attachment and well-spread morphology of the osteoblast over the scaffold. It was well documented in the literature that the roughness of the scaffold-surface plays a vital role in osteoblast cell attachment and proliferation [60,61]. Thus, the good adhesion of the osteoblast is an outcome of the nano-rough surface provided by the presence of nHAp particles in the scaffold. The ESEM analysis showed the good adhesion and high proliferation rate of osteoblasts over nHAp–chitosan–gelatin–alginate scaffold. This result was also corroborated with MTT assay, which confirmed the potential of nHAp–chitosan–gelatin–alginate composite scaffold towards bone tissue engineering.

Fig. 10 illustrated the phase contrast microscopy of the cell–scaffold construct that showed the viable and healthy cells which increased in density with incubation time. This result supported the MTT assay result and also revealed increased cell proliferation with the incubation time. The osteoblast cells showed polygonal and spindle shaped morphology and the cells are well-spread over the surface of the composite scaffold.

Overall, the result of cell viability and attachment study showed that the nHAp–chitosan–gelatin–alginate composite scaffold provided a well-suited environment for the adherence and proliferation of osteoblast cells. Thus, it can be a good candidate for bone regeneration and better scaffold compared to the chitosan–gelatin–alginate scaffold.

In this article, we restricted our study for in vitro studies related to scaffold and its behavior when seeded with osteoblast cells. Before using a scaffold for clinical trial, the scaffold will be immersed in a culture medium (e.g., DMEM) for sufficient time, to allow maximum swelling of the scaffold. After maximum swelling, when the scaffold is subjected for clinical trial it is expected that there will be no further swelling of scaffold when implanted at a site of defect in the body.

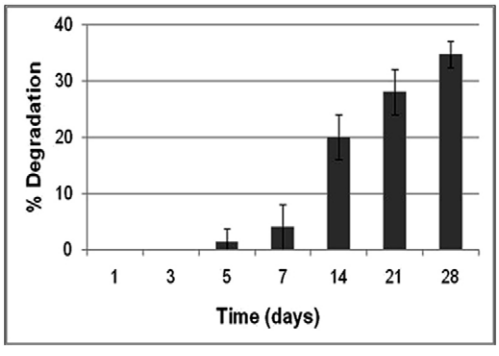

Fig. 7. Percentage degradation of nHAp–chitosan–gelatin–alginate composite scaffold in lysozyme–PBS solution.

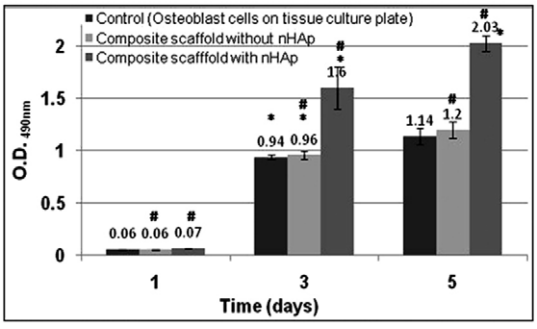

Fig. 8. Viability of osteoblast cells over nHAp–chitosan–gelatin–alginate composite scaffolds at 1, 3 and 5 days, respectively. Here, O.D. is directly proportional to the cell viability. (*) stands for significant difference between control and scaffold on the same culture day ($p < 0.05$); (#) represents significant difference between the same scaffold on different culture days ($p < 0.05$).

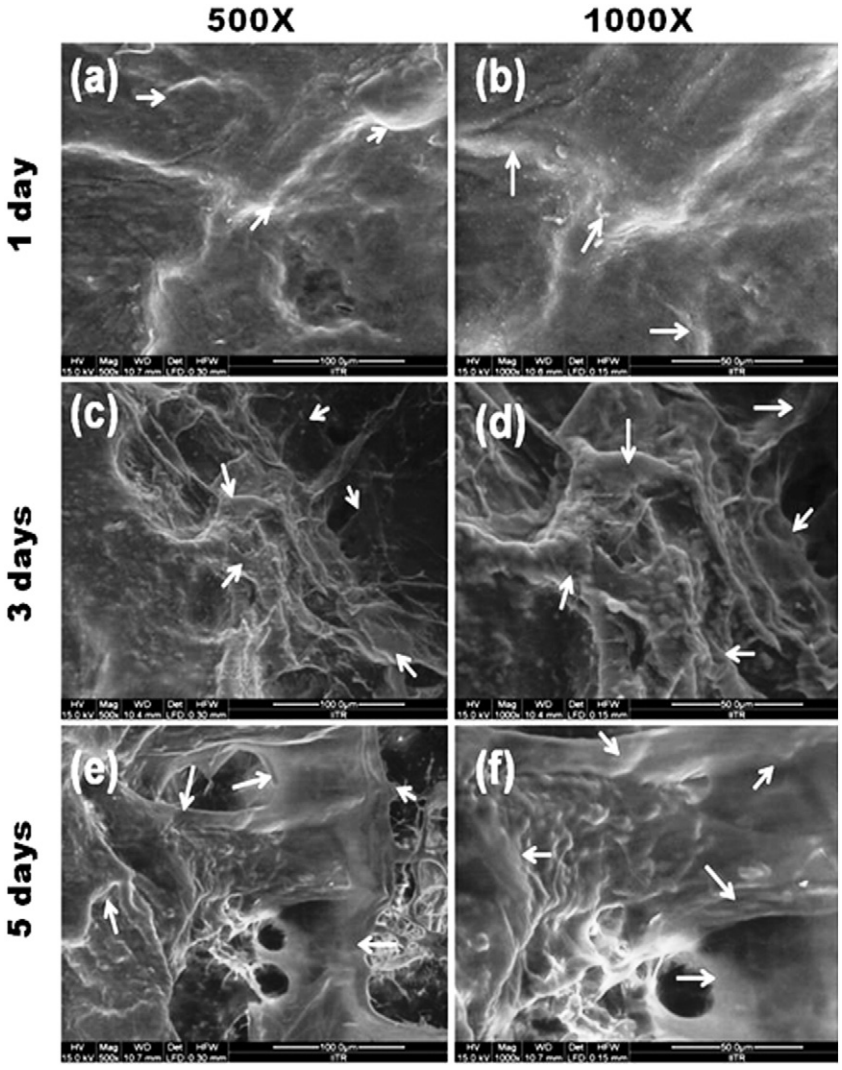

Fig. 9. ESEM images of osteoblast cells cultured on nHAp–chitosan–gelatin–alginate composite scaffold. White arrows indicate the cells over the scaffold.

However, it will be proved only after clinical trial. If someway some problem is created due to the size of the scaffold during clinical trial, we will control the size of the scaffold to solve the problem. Scaffold (swelled) size will be selected as per the size of the tissue defect.

3.9.2. Histological staining of cell–scaffold construct

Osteoblast cells incubated with the nHAp–chitosan–gelatin–alginate composite scaffold stained Alizarin Red positive as shown in Fig. 11(A). Alizarin Red staining has the greatest sensitivity for the detection of calcium pyrophosphate crystals which is an indication of mineralization. The calcium deposition was observed as reddish-black spots by Alizarin Red histological staining. The mineralization seen in Alizarin Red staining of the cells implies that these cells have good osteogenic potential over the scaffold. A similar result was obtained by Huang and coworkers, upon staining the mesenchymal stem cells over the hydrogel scaffold with Alizarin Red for exploring their osteogenic potential [40]. The osteoblast cells also showed positive Giemsa staining which reveals the presence of large cells with prominent spherical nuclei as expected and reported by other scientists [41]. However, osteoblasts were not stained by Oil Red staining indicating that they were not differentiated in vitro into adipocyte cells and retained their osteoblastic phenotype in the presence of the scaffold. The results of histological staining further support the growth and viability of osteoblasts over the scaffold, thereby proving the great prospective of this scaffold for bone tissue engineering applications.

3.9.3. Molecular marker expression in osteoblast cells in the presence and absence of scaffold

In the present work, we have seen the effect of the nHAp–chitosan–gelatin–alginate composite scaffold on expression of specific genes in human osteoblast (bone) cells. These cells normally expressed CD105 and CD73 as mesenchymal markers and showed negative expression for CD34 which is a hematopoietic marker. These cells also expressed CD44, Keratin 18 and osteocalcin (OCN), which is a one of the specific markers for osteoblastic phenotype. Osteocalcin is secreted solely by osteoblasts, and plays an important role in the body's metabolic regulation [62].

We found that human osteoblast cells expressed all these genes i.e., CD105, CD73, CD44 and OCN in the presence and absence of the scaffold as shown in Fig. 12. Tsukita et al. have shown that CD44 is a cell-surface protein (adhesion receptor) involved in proper cell–cell and cell–scaffold interaction [63]. Our experiment has clearly shown high expression of CD44 by osteoblast cells seeded over the scaffold, indicating the proper interaction between the cells and the extracellular matrix proteins present in the scaffold. The expressions of OCN in osteoblast cells (in the presence or absence of scaffold) have indicated the well maintenance of osteoblastic phenotype of these cells even in the presence of the scaffold. As OCN is secreted solely by the osteoblast cells [64], the OCN gene expression seen (in this study) in the osteoblast cells with and without scaffold clearly signifies that the cells maintained their osteoblastic potential even in the presence of the scaffold and

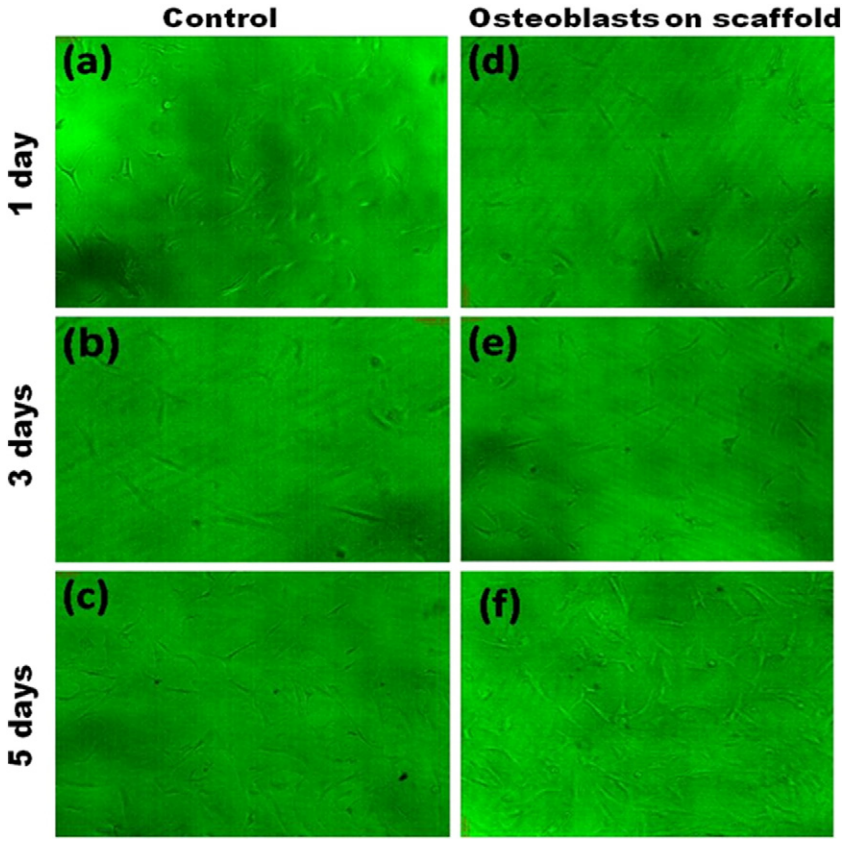

Fig. 10. Phase contrast microscopy of osteoblast cells–scaffold construct (magnification: 10X for all images).

therefore the nHAp–chitosan–gelatin–alginate scaffold can serve as a good substrate for bone regeneration. Keratin 18 is a differentiating marker, which also showed normal expression in the osteoblast cells in the presence of the scaffold indicating that osteoblast cells well maintained their phenotype in this fabricated scaffold. Recently, several studies have shown the importance of the use of mesenchymal stem cells (MSCs) in regenerative medicine for the cure of many diseases [65, 66]. Human osteoblast cells used in this study, also expressed mesenchymal stem cell markers i.e., CD105 and CD73 in the presence of scaffold indicating that these cells in the presence of scaffold have potentiality to enhance bone regenerative process.

4. Conclusions

The nHAp–chitosan–gelatin–alginate composite scaffold was successfully fabricated by the foaming method, without using any surfactant. This polymer combination helped in stabilizing foam for a long time, which brought the success of scaffold fabrication by the foaming method. The inclusion of nanoparticles of hydroxyapatite into the scaffold matrix imparted a good mechanical stability and created a nanotopographic rough surface that enhanced adhesion and proliferation of osteoblasts. The good hydrophilicity of the scaffold as depicted by swelling ratio indicates that the scaffold will facilitate the absorption

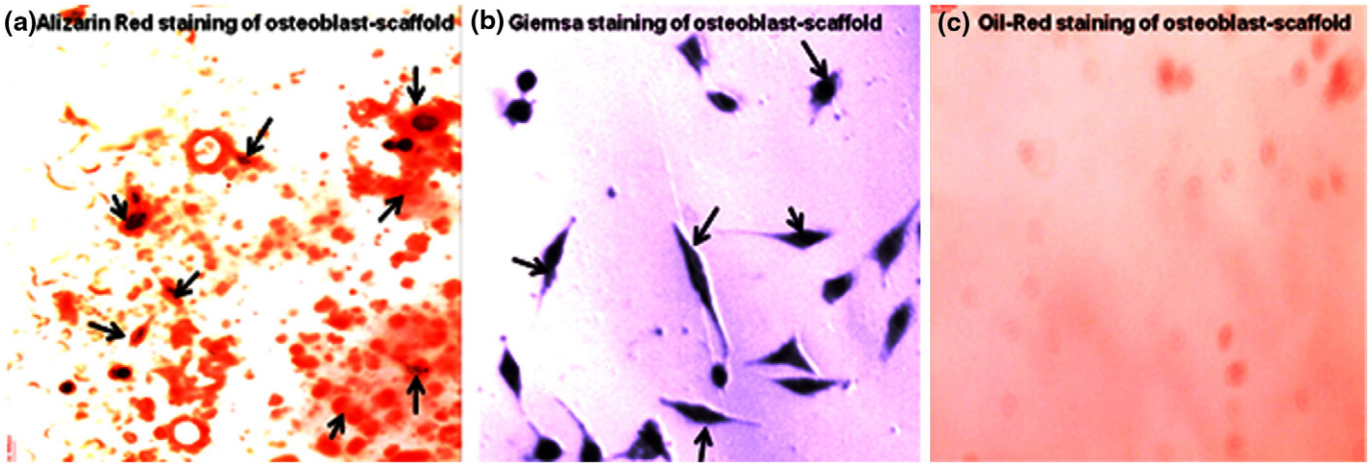

Fig. 11. Alizarin Red, Giemsa and Oil Red staining of osteoblasts (A,B,C) after 5 days of incubation with nHAp–chitosan–gelatin–alginate composite scaffold (magnification: 20X). Osteoblast stains positive for both Alizarin Red and Giemsa stain (A,B). Osteoblast stains Oil Red negative (C). Red color indicated by arrows in (A) shows calcium deposition. Black arrows indicate the cells present over the scaffold.

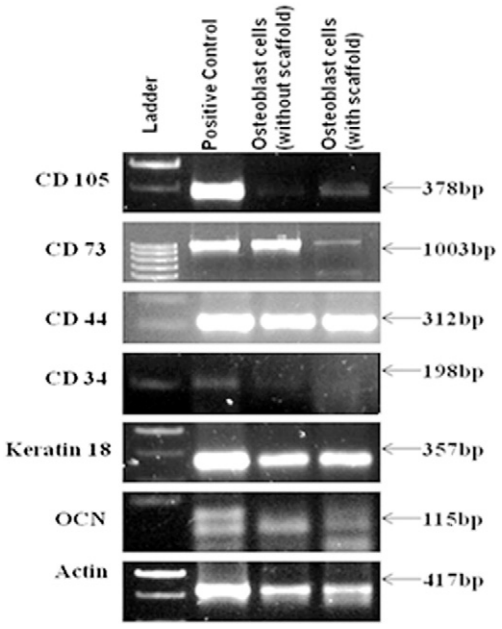

Fig. 12. Gene expression studies for osteoblast cells in the presence and in the absence of nHAp–chitosan–gelatin–alginate composite scaffold.

of body fluid and nutrient diffusion. The prolonged degradation time provided by the addition of nHAp in the composite scaffold might be a feature that offers sufficient time for the formation of neotissue and ECM. The results of the in vitro cell culture studies and gene expression by seeding osteoblast cells over the scaffold signify that the newly developed nHAp based composite scaffold is a good scaffold for osteoblast attachment and proliferation, thus it can be potentially applied for bone regeneration.

Conflict of interest

The authors wish to confirm that there are no known conflicts of interest associated with this publication.

Acknowledgements

The authors are grateful to the Council of Scientific and Industrial Research (Grant No. 27(0222)/10/EM R-II dated 31.05.10), as well as Ministry of Human Resources and Development (MHRD), India, for funding this research work. We are thankful to the Management of Jaslok Hospital and Research Centre, Mumbai for providing facilities to do tissue culture work and Mr. Sachin Ramdas Chaugule, Research Assistant, Dept. of Molecular Medicine and Biology, for his cooperation in carrying out the biocompatibility experiments.

References

[1] A.R.C. Pinto, R.L. Reis, N.M. Neves, Scaffolds based bone tissue engineering: the role of chitosan, Tissue Eng. Part B Rev. 17 (2011) 331–347.
[2] A. Agarwal, Advent and maturation of regenerative medicine, Tissue Eng. Regen. Med. 10 (2013) 155–159.
[3] D. Lickorish, L. Guan, J.E. Davies, A three-phase, fully resorbable, polyester/calcium phosphate scaffold for bone tissue engineering: evolution of scaffold design, Biomaterials 28 (2007) 1495–1502.
[4] P.S. Thomas, S. Thomas, S. Bandyopadhyay, A. Wurm, C. Schick, Polystyrene/calcium phosphate nanocomposites: dynamic mechanical and differential scanning calorimetric studies, Combust. Sci. Technol. 68 (2008) 3220–3229.
[5] P.S. Thomas, S. Thomas, N.E. Zafeiropoulos, S. Bandyopadhyay, A. Wurm, C. Schick, Polystyrene/calcium phosphate nanocomposites: morphology, mechanical, and dielectric properties, Polym. Eng. Sci. 52 (2012) 689–699.
[6] M.B. Yaylaoglu, C. Yildiz, F. Korkusuz, V. Hasirci, A novel osteochondral implant, Biomaterials 20 (1999) 1513–1520.
[7] J.B. Park, Y.S. Kim, G. Lee, B.G. Yun, C.H. Kim, The effect of surface treatment of titanium with sand-blasting/acid-etching or hydroxyapatite-coating and application of bone morphogenetic protein-2 on attachment, proliferation, and differentiation of stem cells derived from buccal fat pad, Tissue Eng. Regen. Med. 10 (2013) 115–121.
[8] C. Sharma, A.K. Dinda, N.C. Mishra, Synthesis and characterization of glycine modified chitosan–gelatin–alginate composite scaffold for tissue engineering applications, J. Biomater. Tissue Eng. 2 (2012) 133–142.
[9] S. Gautam, A.K. Dinda, N.C. Mishra, Fabrication and characterization of PCL/gelatin composite nanofibrous scaffold for tissue engineering applications by electrospinning method, Mater. Sci. Eng. C 33 (2013) 1228–1235.
[10] S. Gautam, C.F. Chou, A.K. Dinda, P.D. Potdar, N.C. Mishra, Surface modification of nanofibrous polycaprolactone/gelatin composite scaffold by collagen I grafting for skin tissue engineering, Mater. Sci. Eng. C 34 (2014) 402–409.
[11] C. Sharma, S. Gautam, A.K. Dinda, N.C. Mishra, Cartilage tissue engineering: current scenario and challenges, Adv. Mater. Lett. 2 (2011) 90–99.
[12] C. Sharma, A.K. Dinda, N.C. Mishra, Fabrication and characterization of natural origin chitosan–gelatin–alginate composite scaffold by foaming method without using surfactant, J. Appl. Polym. Sci. 127 (2013) 3228–3241.
[13] S. Gautam, C.F. Chou, A.K. Dinda, P.D. Potdar, N.C. Mishra, Fabrication and characterization of PCL/gelatin/chitosan ternary nanofibrous composite scaffold for tissue engineering applications, J. Mater. Sci. 49 (2014) 1076–1089.
[14] R. Dorati, C. Colonna, I. Genta, A. De Trizio, T. Modena, H. Klöss, B. Conti, In vitro characterization of an injectable in situ forming composite system for bone reconstruction, Polym. Degrad. Stab. 119 (2015) 151–158.
[15] S. Gupta, C. Sharma, A.K. Dinda, A.K. Ray, N.C. Mishra, Tooth tissue engineering: potential and pitfalls, J. Biomimetics Biomater. Tissue Eng. 12 (2011) 59–81.
[16] S.K. Gupta, P.D. Potdar, A.K. Dinda, N.C. Mishra, Surface modified goat-lung decellularized scaffold for bio-artificial skin tissue engineering applications, J. Biomater. Tissue Eng. 3 (2013) 1–9.
[17] S.K. Gupta, A.K. Dinda, P.D. Potdar, N.C. Mishra, Fabrication and characterization of scaffold from cadaver goat-lung tissue for skin tissue engineering applications, Mater. Sci. Eng. C 33 (2013) 4032–4038.
[18] S.K. Gupta, A.K. Dinda, P.D. Potdar, N.C. Mishra, Modification of decellularized goat-lung scaffold with chitosan/nanohydroxyapatite composite for bone tissue engineering applications, Biomed. Res. Int. 2013 (2013) 1–11.
[19] C. Isikli, V. Hasirci, N. Hasirci, Development of porous chitosan–gelatin/hydroxyapatite composite scaffolds for hard tissue-engineering applications, J. Tissue Eng. Regen. Med. 6 (2012) 135–143.
[20] E. Sachlos, J.T. Czernuszka, Making tissue engineering scaffolds work. Review: the application of solid freeform fabrication technology to the production of tissue engineering scaffolds, Eur. Cell. Mater. 5 (2003) 39–40.
[21] Lin KH, Mishra N, Liu YL, Wang CC, Fabricating scaffolds and other cell-growth structures using microfluidics to culture biological samples, US Patent Pub. No.·US20110091972 (21.04.11)
[22] P. Eiselt, J. Yeh, R.K. Latvala, L.D. Shea, D.J. Mooney, Porous carriers for biomedical applications based on alginate hydrogels, Biomaterials 21 (2000) 1921–1927.
[23] M. Swetha, K. Sahithi, A. Moorthi, N. Srinivasan, K. Ramasam, N. Selvamurugan, Biocomposites containing natural polymers and hydroxyapatite for bone tissue engineering, Int. J. Biol. Macromol. 47 (2010) 1–4.
[24] K.S. Katti, D.R. Katti, R. Dash, Synthesis and characterization of a novel chitosan/montmorillonite/hydroxyapatite nanocomposite for bone tissue engineering, Biomed. Mater. 3 (2008) 034122.
[25] V.K. Mourya, N.N. Inamdara, A. Tiwari, Carboxymethyl chitosan and its applications, Adv. Mater. Lett. 1 (2010) 11–33.
[26] J.P. Zheng, C.Z. Wang, X.X. Wang, H.Y. Wang, H. Zhuang, K.D. Yao, Preparation of biomimetic three-dimensional gelatin/montmorillonite–chitosan scaffold for tissue engineering, React. Funct. Polym. 67 (2007) 780–788.
[27] R. Ramya, J. Venkatesan, S.K. Kim, P.N. Sudha, Biomedical applications of chitosan: an overview, J. Biomater. Tissue Eng. 2 (2012) 100–111.
[28] R. Gu, W. Sun, H. Zhou, Z. Wu, Z. Meng, X. Zhu, Q. Tang, The performance of a fly-larva shell-derived chitosan sponge as an absorbable surgical hemostatic agent, Biomaterials 31 (2010) 1270–1277.
[29] Y.P. Yun, S.Y. Lee, H.J. Kim, J.J. Song, S.E. Kim, Improvement of osteoblast functions by sustained release of bone morphogenetic protein-2 (BMP-2) from heparin-coated chitosan scaffold, Tissue Eng. Regen. Med. 10 (2013) 183–191.
[30] W.W. Thein-Han, R.D.K. Misra, Biomimetic chitosan–nanohydroxyapatite composite scaffolds for bone tissue engineering, Acta Biomater. 5 (2009) 1182–1197.
[31] G.A. Silva, P. Ducheyne, R.L. Reis, Materials in particulate form for tissue engineering. Basic concepts, J. Tissue Eng. Regen. Med. 1 (2007) 4–24.
[32] K.S.V. Rao, I. Chung, C.S. Ha, Synthesis and characterization of poly(acrylamidoglycolic acid) grafted onto chitosan and its polyelectrolyte complexes with hydroxyapatite, React. Funct. Polym. 68 (2008) 943–953.
[33] J.L. Drury, R.G. Dennis, D.J. Mooney, The tensile properties of alginate hydrogels, Biomaterials 25 (2004) 3187–3199.
[34] Y. Li, T. Liu, J. Zheng, X. Xu, Glutaraldehyde crosslinked chitosan/hydroxyapatite bone repair scaffold and its application as drug carrier for icariin, J. Appl. Polym. Sci. 130 (3) (2013) 1539–1547.
[35] Y. Liu, M. An, L. Wang, H. Qiu, Preparation and characterization of chitosan–gelatin/glutaraldehyde scaffolds, J. Macromol. Sci., Part B: Phys. 53 (2) (2014) 309–325.
[36] V. Karageorgiou, D. Kaplan, Porosity of 3D biomaterial scaffolds and osteogenesis, Biomaterials 26 (2005) 5474–5491.
[37] G. Orive, R.M. Hernandez, A.R. Gascon, M. Igartua, A. Rojas, J.L. Pedraz, Development and optimisation of alginate–PMCG–alginate microcapsules for cell immobilization, Int. J. Pharm. 259 (2003) 57–68.

[38] L. Ma, C. Gao, Z. Mao, J. Zhou, J. Shen, X. Hu, C. Han, Collagen/chitosan porous scaffolds with improved biostability for skin tissue engineering, Biomaterials 24 (2003) 4833–4841.
[39] C. Tangsadthakun, S. Kanokpanont, N. Sanchavanchavanalit, T. Banaprasert, S. Damrongsakkul, Properties of collagen/chitosan scaffolds for skin tissue engineering, J. Met. Mater. Min. 16 (2006) 37–44.
[40] G.T.J. Huang, K. Shagramanova, S.W. Chan, Formation of odontoblast-like cells from cultured human dental pulp cells on dentin in vitro, J. Endod. 32 (2006) 1066–1073.
[41] R.A. Kadir, S.H.Z. Ariffin, R.M.A. Wahab, S. Senafi, F.Z. Huyop, Differentiation potential of human suspension mononucleated peripheral blood cells, Afr. J. Biotechnol. 10 (2011) 10756–10764.
[42] P.D. Potdar, R.P. Subedi, Defining Molecular Phenotypes of Mesenchymal and hematopoietic Stem Cells derived from Peripheral blood of Acute Lymphocytic Leukemia patients for regenerative stem cell therapy, J. Stem Cells 7 (2011) 29–40.
[43] P. Potdar, J. Sutar, Establishment and molecular characterization of mesenchymal stem cell lines derived from human visceral and subcutaneous adipose tissues, J. Stem Cell Regen Med 6 (2010) 26–35.
[44] P.D. Potdar, S.B. D'souza, Isolation of Oct4+, Nanog+ and SOX2− mesenchymal cells from peripheral blood of a diabetes mellitus patient, Hum. Cell 24 (2011) 51–55.
[45] X. Shi, Y. Du, L. Sun, B. Zhang, A. Dou, Polyelectrolyte complex beads composed of water-soluble chitosan/alginate: characterization and their protein release behavior, J. Appl. Polym. Sci. 100 (2006) 4614–4622.
[46] J. Berger, M. Reist, J.M. Mayer, O. Felt, N.A. Peppas, R. Gurny, Structure and interactions in covalently and ionically crosslinked chitosan hydrogels for biomedical applications, Eur. J. Pharm. Biopharm. 57 (2004) 19–34.
[47] Y.J. Yin, F. Zhao, X.F. Song, K.D. Yao, W.W. Lu, J.C. Leong, Preparation and characterization of hydroxyapatite/chitosan–gelatin network composite, J. Appl. Polym. Sci. 77 (2000) 2929–2938.
[48] M. Rajkumar, K. Kavitha, M. Prabhu, N. Meenakshisundaram, V. Rajendran, Nanohydroxyapatite–chitosan–gelatin polyelectrolyte complex with enhanced mechanical and bioactivity, Mater. Sci. Eng. C 33 (2013) 3237–3244.
[49] K.A. Hing, B. Annaz, S. Saeed, P.A. Revell, T. Buckland, Microporosity enhances bioactivity of synthetic bone graft substitutes, J. Mater. Sci. Mater. Med. 16 (2005) 467–475.
[50] S.K. Lan Levengood, S.J. Polak, M.B. Wheeler, A.J. Maki, S.G. Clark, R.D. Jamison, A.J. Wagoner Johnson, Multiscale osteointegration as a new paradigm for the design of calcium phosphate scaffolds for bone regeneration, Biomaterials 31 (2010) 3552–3563.
[51] H.W. Kim, J.C. Knowles, H.E. Kim, Hydroxyapatite and gelatin composite foams processed via novel freeze-drying and crosslinking for use as temporary hard tissue scaffolds, J. Biomed. Mater. Res. A 72 (2004) 136–145.
[52] N. Pramanik, D. Mishra, I. Banerjee, T.K. Maiti, P. Bhargava, P. Pramanik, Chemical synthesis, characterization, and biocompatibility study of hydroxyapatite/chitosan phosphate nanocomposite for bone tissue engineering applications, Int. J. Biomater. 2009 (2009) 1–8.
[53] J. Venkatesan, Z.J. Qian, B. Ryu, N.A. Kumar, S.K. Kim, Preparation and characterization of carbon nanotube-grafted-chitosan — natural hydroxyapatite composite for bone tissue engineering, Carbohydr. Polym. 83 (2011) 569–577.
[54] O. Im, J. Li, M. Wang, L.G. Zhang, M. Keidar, Biomimetic three-dimensional nanocrystalline hydroxyapatite and magnetically synthesized single-walled carbon nanotube chitosan nanocomposite for bone regeneration, Int. J. Nanomedicine 7 (2012) 2087–2099.
[55] J.M. Grech, J.F. Mano, R.L. Reis, Processing and characterization of chitosan microspheres to be used as templates for layer-by-layer assembly, J. Mater. Sci. Mater. Med. 21 (2010) 1855–1865.
[56] B.Y. Choi, H.J. Park, S.J. Hwang, J.B. Park, Preparation of alginate beads for floating drug delivery system: effects of CO_2 gas-forming agents, Int. J. Pharm. 239 (2002) 81–91.
[57] K.R. Mohamed, A.A. Mostafa, Preparation and bioactivity evaluation of hydroxyapatite–titania/chitosan–gelatin polymeric biocomposites, Mater. Sci. Eng. C 28 (2008) 1087–1099.
[58] M. Peter, N.S. Binulal, S.V. Nair, N. Selvamurugan, H. Tamura, R. Jayakumar, Novel biodegradable chitosan–gelatin/nano-bioactive glass ceramic composite scaffolds for alveolar bone tissue engineering, Chem. Eng. J. 158 (2010) 353–361.
[59] Y. Yang, J. Tian, L. Deng, J.L. Ong, Morphological behavior of osteoblast-like cells on surface-modified titanium in vitro, Biomaterials 23 (2002) 1383–1389.
[60] D. Gupta, J. Venugopal, S. Mitra, D.V. Giri, S. Ramakrishna, Nanostructured biocomposite substrates by electrospinning and electrospraying for the mineralization of osteoblasts, Biomaterials 30 (2009) 2085–2094.
[61] Y. Gao, W.L. Cao, X.Y. Wang, Y.D. Gong, J.M. Tian, N.M. Zhao, X.F. Zhang, Characterization and osteoblast-like cell compatibility of porous scaffolds: bovine hydroxyapatite and novel hydroxyapatite artificial bone, J. Mater. Sci. Mater. Med. 17 (2006) 815–823.
[62] H.Y. Wan, H.Q. Sun, G.X. Sun, X. Li, Z.Z. Shang, The early phase response of rat alveolar bone to traumatic occlusion, Arch. Oral Biol. 57 (2012) 737–743.
[63] Saehiko Tsukita, Kumiko Oishi, Naruki Sato, Junji Sagara, Akihiko Kawai, Shoiehiro Tsuldta, ERM family members as molecular linkers between the cell surface glycoprotein C D 44 and actin-based cytoskeletons, J. Cell Biol. 126 (1994) 391–401.
[64] F. Lumachi, V. Camozzi, V. Tombolan, G. Luisetto, Bone mineral density, osteocalcin, and bone-specific alkaline phosphatase in patients with insulin-dependent diabetes mellitus, Ann. N. Y. Acad. Sci. 1173 (2009) E64–E67.
[65] P.D. Potdar, S. Deshpande, Mesenchymal stem cell transplantation: new avenues for stem cell therapies, J. Transplant. Technol. Res. 3 (2013) 1–16.
[66] P.D. Potdar, N.K. Lotey, Stem cells — a promise to elixir, Enliven: J Stem Cell Regen Med 1 (1) (2014) 003.